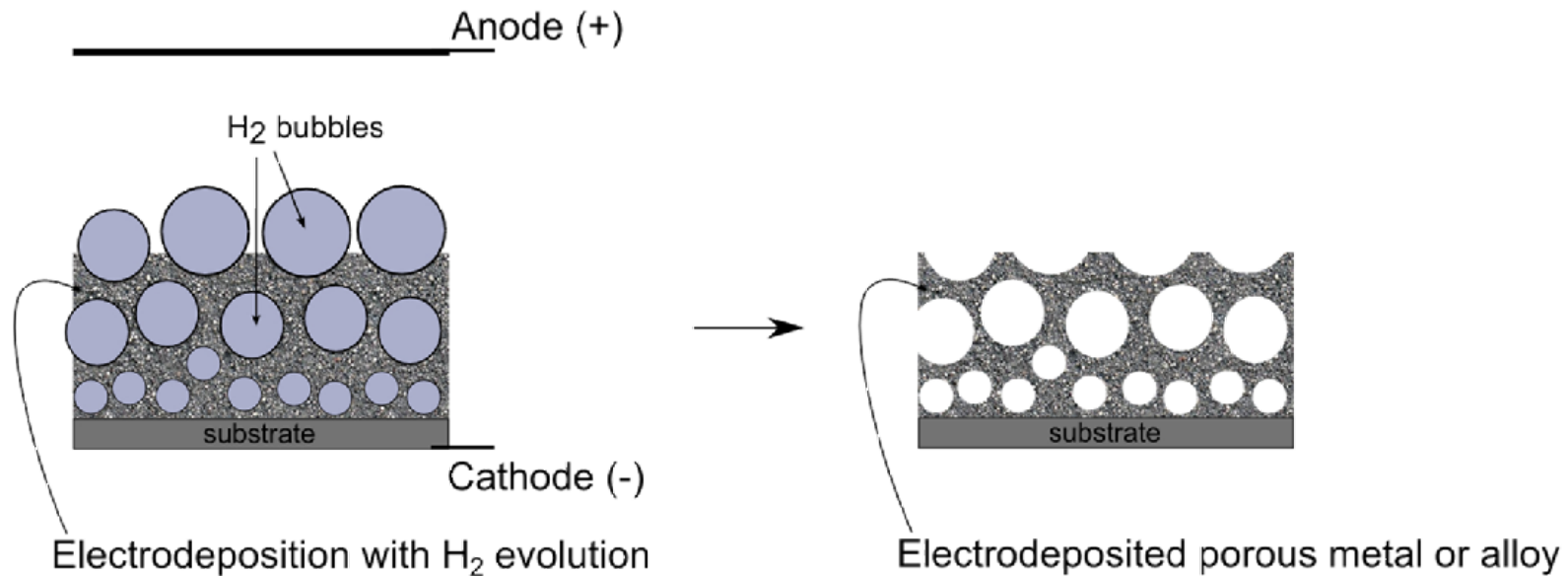


Elettrodeposizione di metalli porosi e leghe metalliche porose: loro applicazioni

L. Mattarozzi, S. Cattarin, N. Comisso, R. Gerbasi,
P. Guerriero, M. Musiani, L. Vázquez-Gómez, E. Verlato

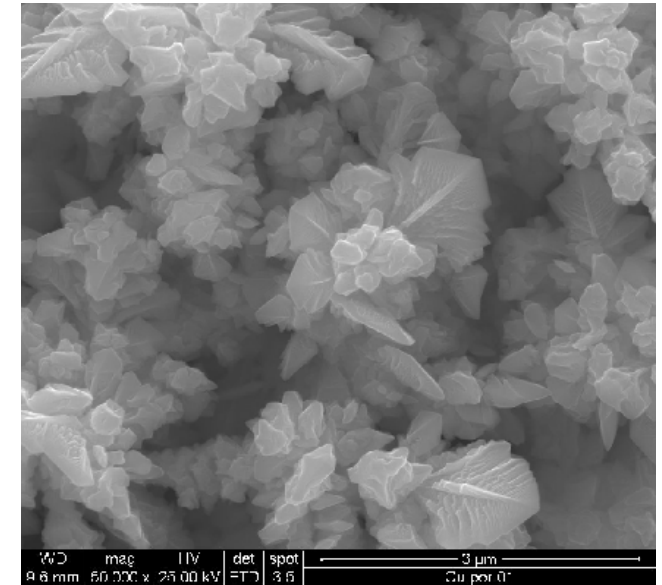
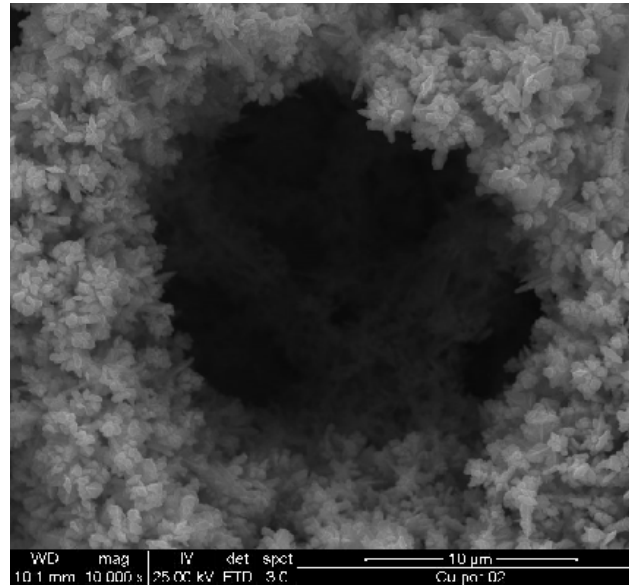
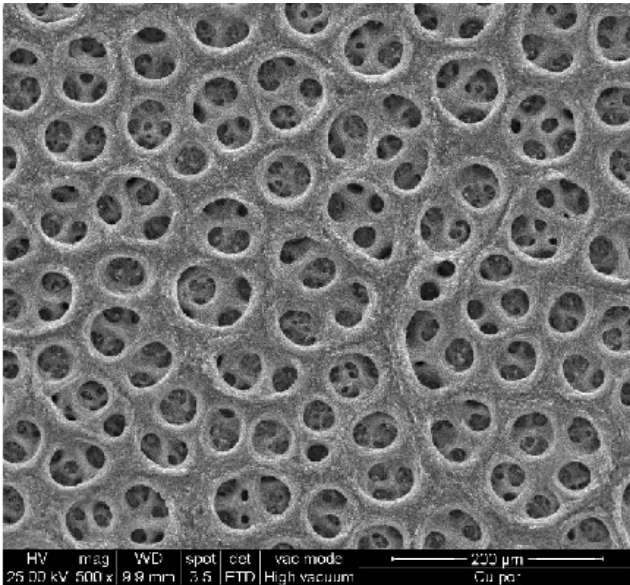
IENI / ICMATE - CNR, Padova, Italy

Hydrogen bubble templated electrodeposition: formation of macropores



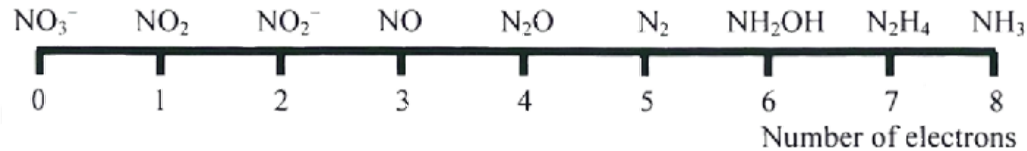
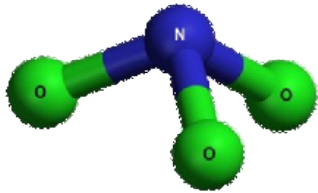
- Hydrogen bubbles act as a faint template that disappears on switching off the current;
- Shape and dimensions of pores depend on bubbles formation-coalescence-detachment;
- No template dissolution is required, the porous material is ready in one step;
- In most electrochemical applications
 - a) the relative lack of order in the deposit is not a limitation;
 - b) the increasing dimensions of pores from substrate towards solution is an advantage.

Hydrogen bubble templated electrodeposition: bimodal porosity



- The material shows macro-pores with a diameter in the range of several tens of microns;
- The “full” part of the deposit has a spongy structure, with a number of tiny dendrites and a large surface area exposed to the electrolyte (f_r in the order of hundreds);
- These properties should promote transport and kinetics (respectively) when the material is used as electrode.

Porous Cu alloys for the electrochemical reduction of nitrates



Electrochemical reduction of nitrates offers several valuable advantages:

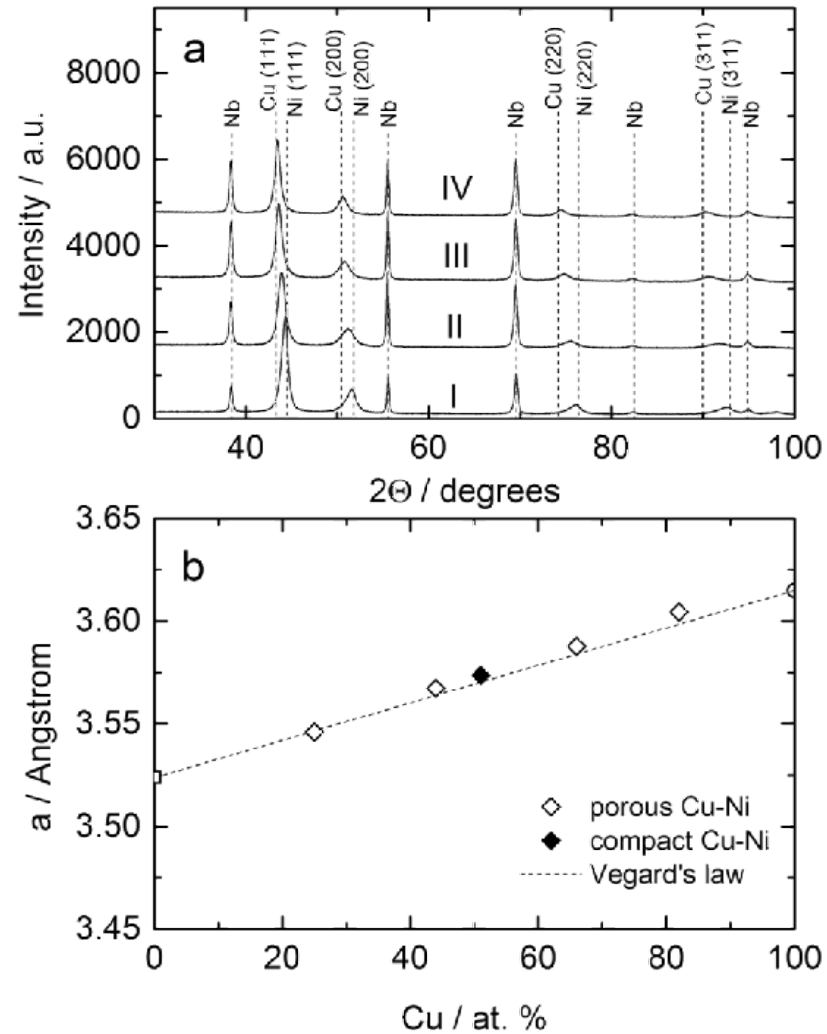
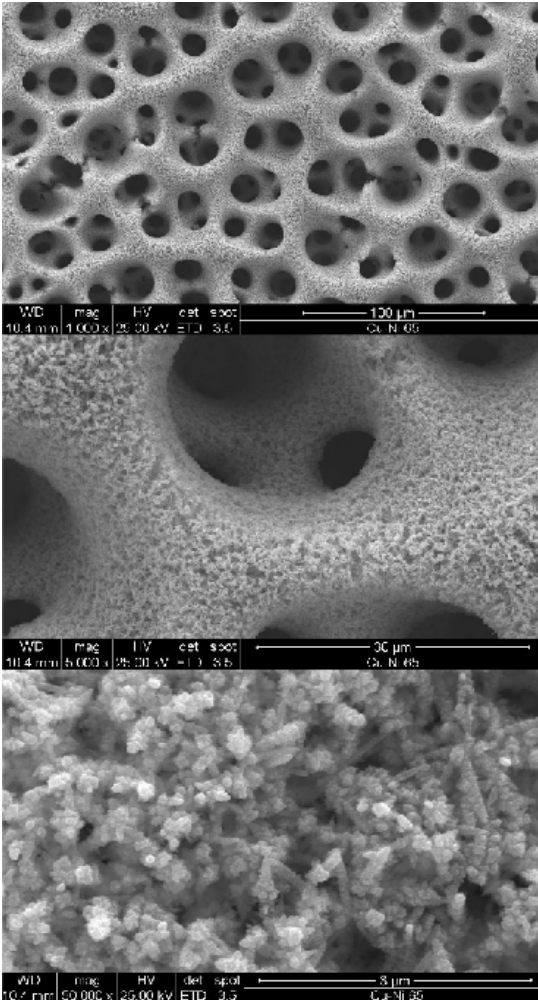
- high treatment efficiency;
- absence of sludge production;
- small equipment and low cost.

In the electrochemical reduction of nitrates in alkali:

- **Cu**, among the non-noble metals, is probably the most efficient;
- **Cu-Ni alloys** offer the additional advantages of **low cost and good corrosion resistance**;
- **Cu-Zn alloys** may offer in principle the advantages of **low cost and low toxicity**.

Electrodeposition of porous Cu-Ni alloy

$\text{Cu}_{70}\text{Ni}_{30}$



I) $\text{Cu}_{25}\text{Ni}_{75}$

II) $\text{Cu}_{44}\text{Ni}_{56}$

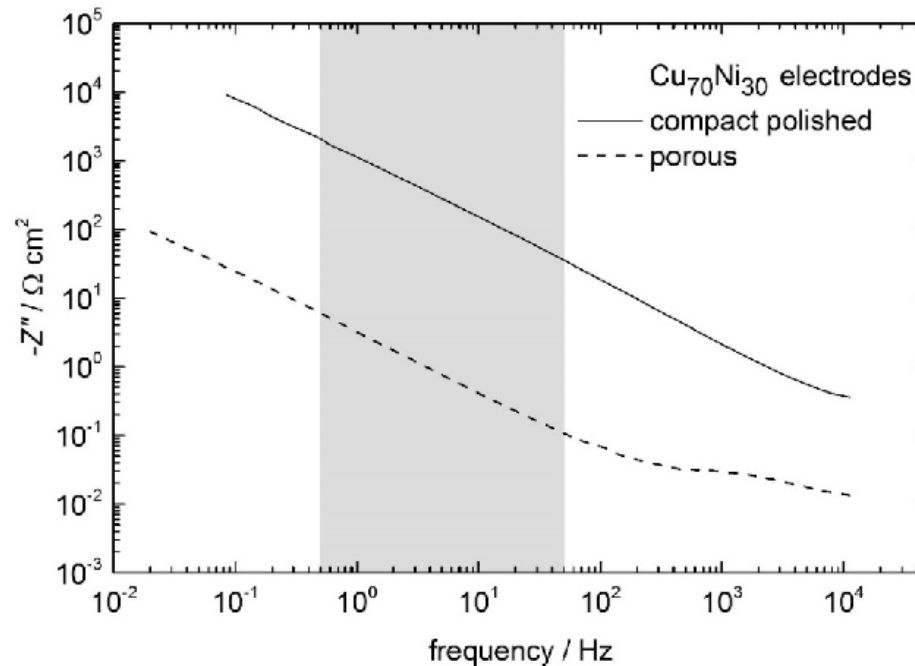
III) $\text{Cu}_{66}\text{Ni}_{34}$

IV) $\text{Cu}_{82}\text{Ni}_{18}$

The alloy composition can be varied over a wide range

The lattice parameter a depends on composition according to Vegard's law

Impedance investigations to estimate the roughness factor



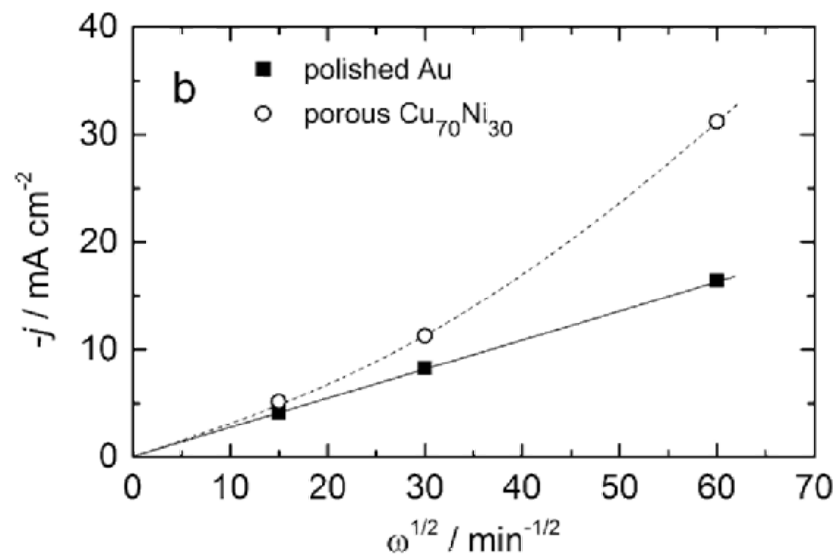
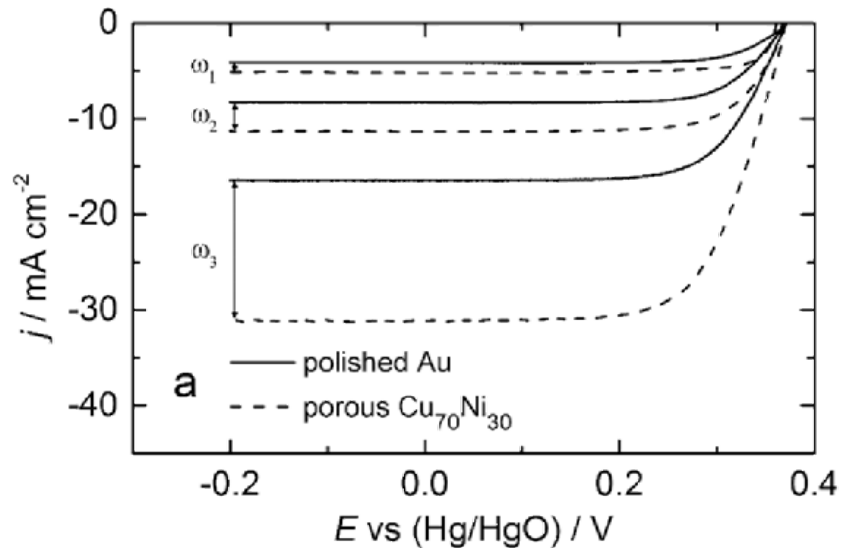
Impedance (EIS) spectra were recorded at a convenient potential $E = -0.7$ V vs (Hg/HgO) where the electrodes showed a blocking behaviour

The surface area of the porous (p) electrode can be estimated from comparison of its impedance response with that of a compact (c) electrode



We can estimate roughness factor $f_r = C_p / C_c \cong (|Z''_c| / |Z''_p|) \cong 360$.

Behaviour of porous Cu-Ni electrodes in a diffusion-controlled process



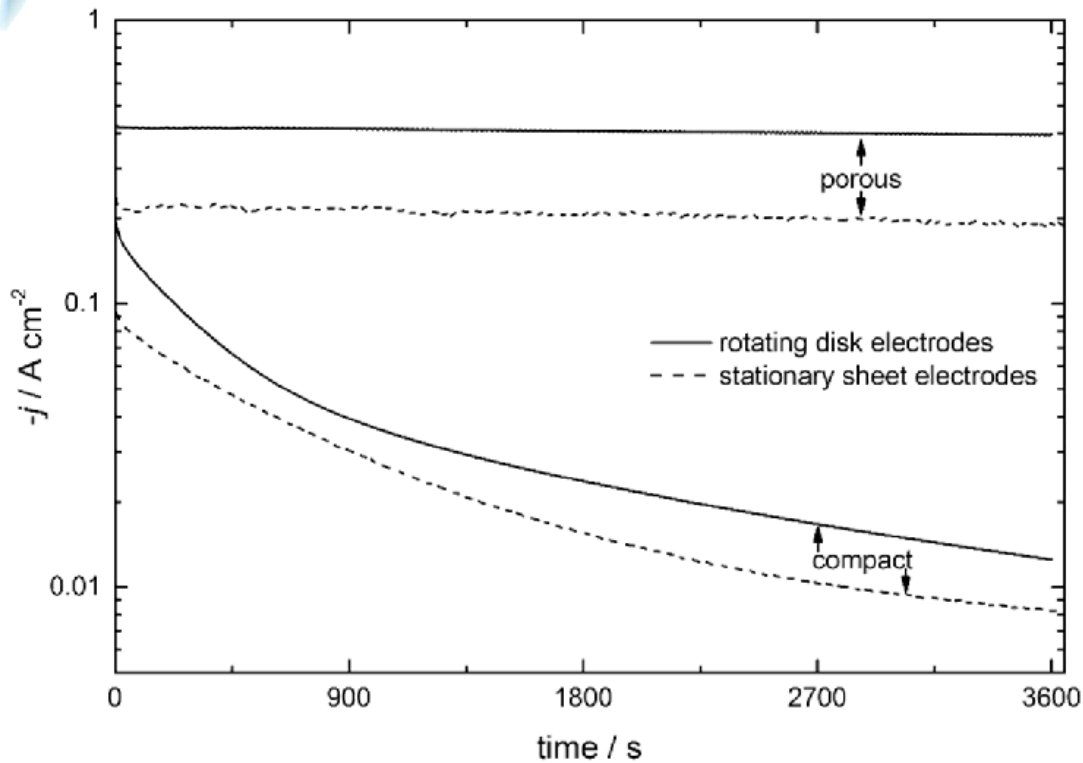
Ferricyanide reduction in alkali at a smooth Au RDE and at a porous $\text{Cu}_{70}\text{Ni}_{30}$ RDE:

- rotation speeds: $\omega_1 = 225$, $\omega_2 = 900$ and $\omega_3 = 3600$ rev min^{-1} .

At variance with flat electrodes (Levich dependence) the plateau current recorded at the porous $\text{Cu}_{70}\text{Ni}_{30}$ electrode increases with $\omega^{1/2}$ in a superlinear way.

Current enhancement may result from more effective convection and/or perfusion of the porous electrode (theory of **Porous Rotating Disk Electrodes**).

Chronoamperometries of NO_3^- reduction



Electrolyte: 0.1 M NO_3^- in 1.0 M NaOH

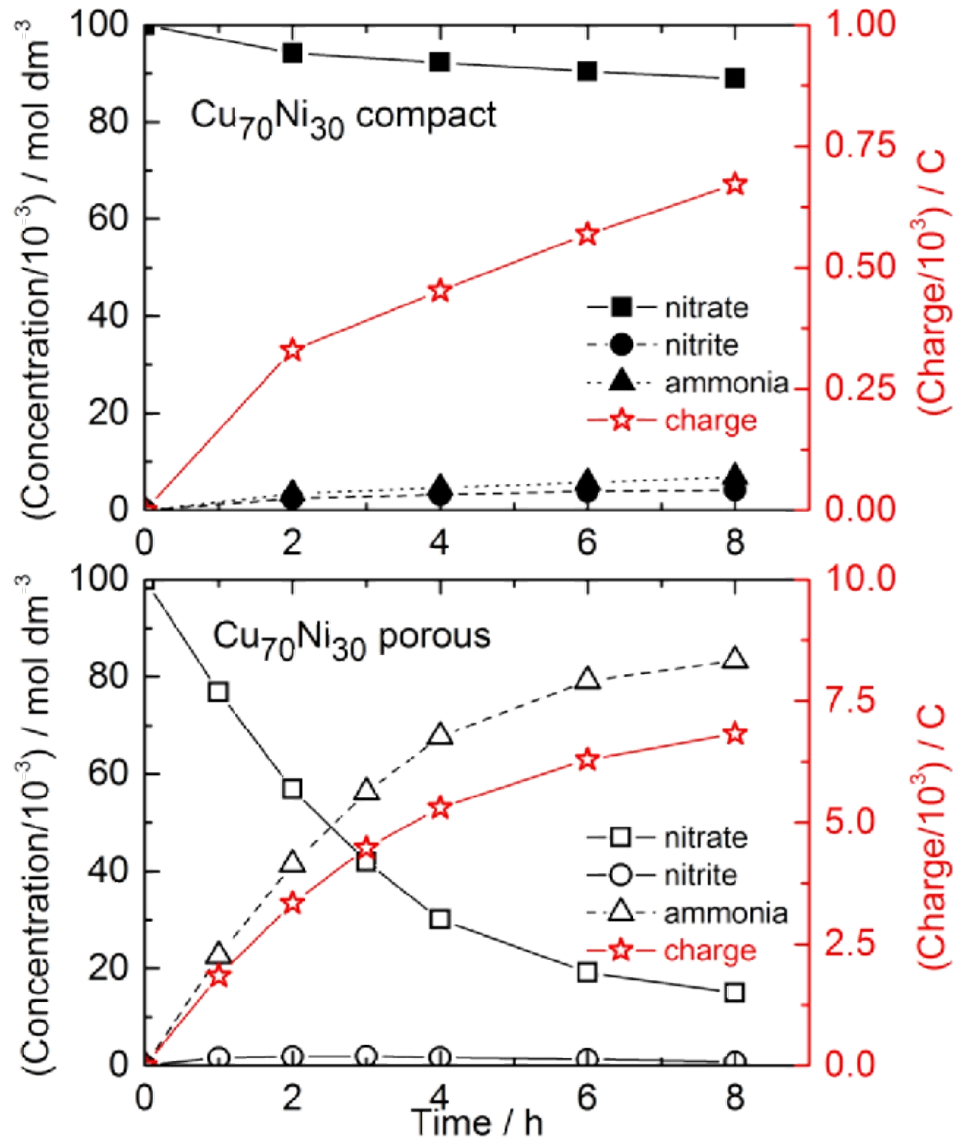
$E = -1.2 \text{ V vs (Hg/HgO)}$

RDE at 900 rev min^{-1} ,

magnetic stirring for sheet electrodes

- The initial current ($t = 0$) is about twice larger at the porous electrode;
- the current is stable at the porous electrodes (unaltered during 1 h) and decays rapidly at the compact ones;
- on this basis, one may expect much faster NO_3^- elimination using the porous electrodes.

Time evolution of the concentration of species during prolonged electrolyses



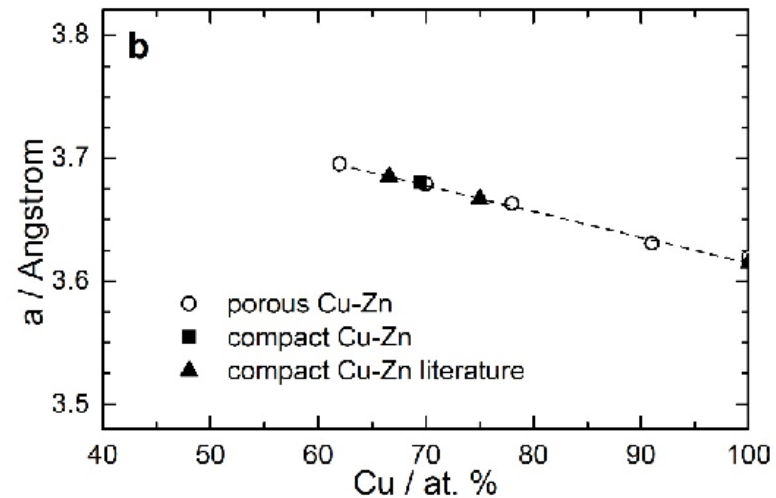
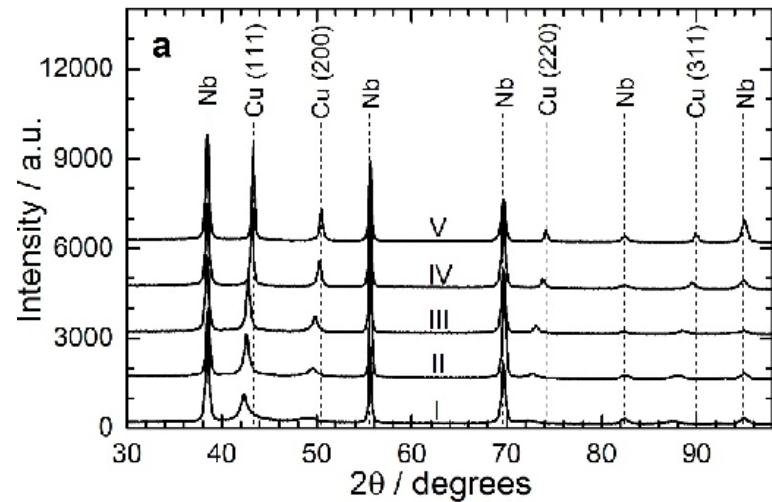
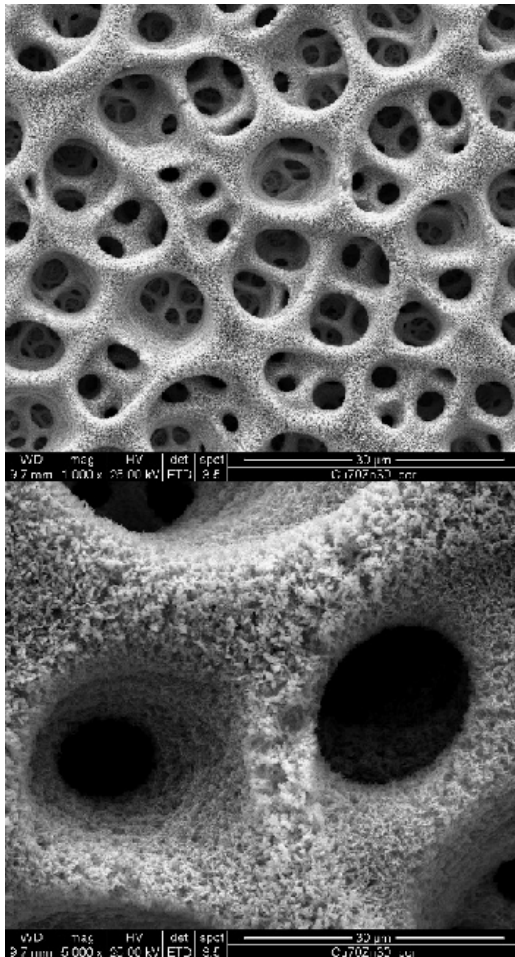
Potentiostatic electrolyses at
 $E = -1.2 \text{ V vs (Hg/HgO)}$

Operating with porous alloy cathodes we obtain:

- much larger reduction charge (about 10x after 8 hours);
- much faster decay of $[\text{NO}_3^-]$ and buildup of $[\text{NH}_3]$;
- better selectivity for the production of a single, dominant product (NH_3).

Electrodeposited porous Cu-Zn alloys

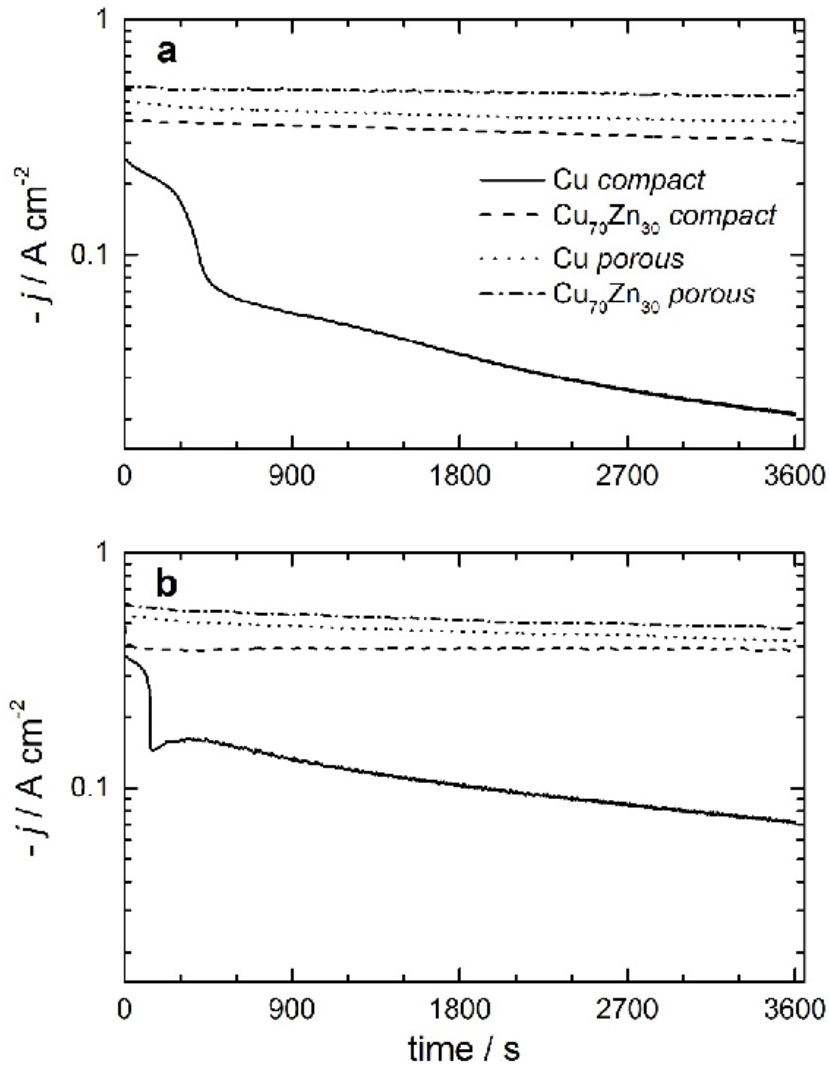
$\text{Cu}_{70}\text{Zn}_{30}$



- I) $\text{Cu}_{63}\text{Zn}_{37}$
- II) $\text{Cu}_{70}\text{Zn}_{30}$;
- III) $\text{Cu}_{79}\text{Zn}_{21}$;
- IV) $\text{Cu}_{90}\text{Zn}_{10}$;
- V) Cu.

- SEM inspection shows morphologic features analogous to those observed for Cu-Ni;
- the cell parameter a varies according to Vegard's law over the investigated composition range.

Chronoamperometries of NO_3^- reduction at Cu and Cu-Zn electrodes



Chronoamperometric curves recorded in
 0.1 M NO_3^- + 1.0 M NaOH, RDE 900 min^{-1} ,

a) $E = -1.4 \text{ V (vs Hg/HgO)}$;

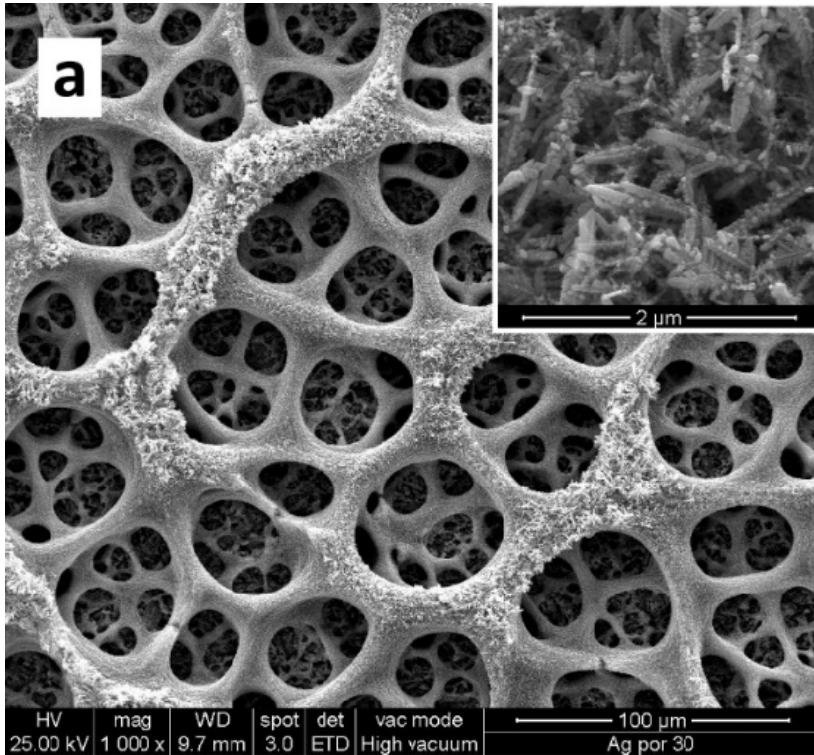
b) $E = -1.6 \text{ V (vs Hg/HgO)}$.

- The initial current is larger:

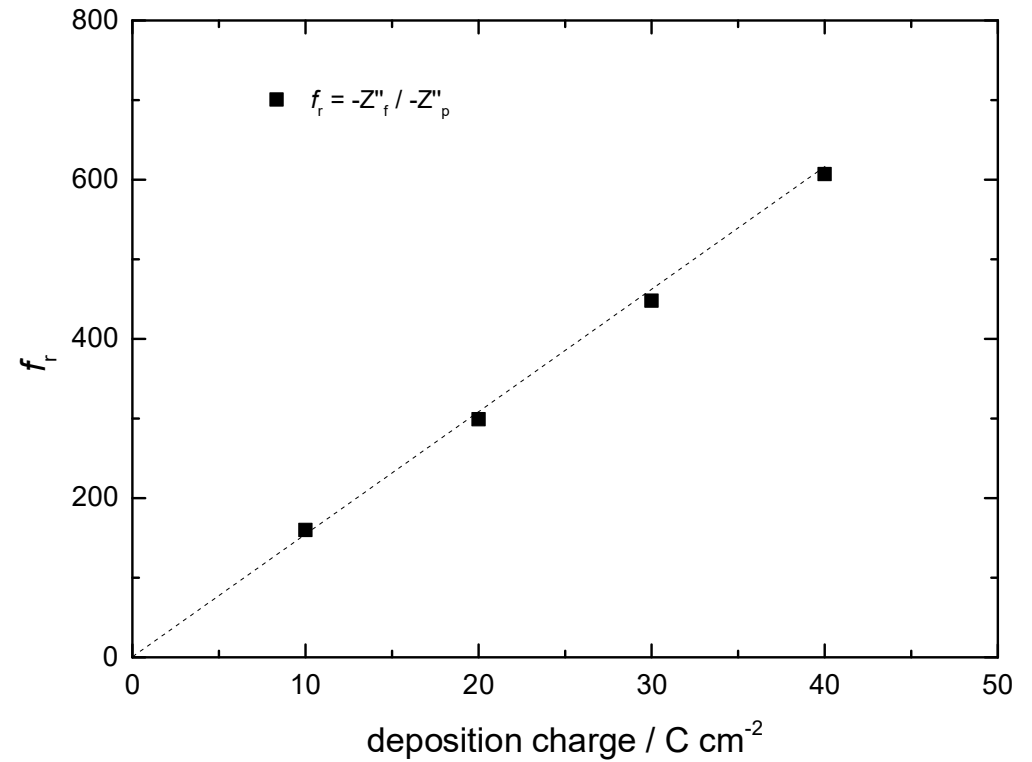
- 1) at alloy electrodes than at Cu;
- 2) at porous than at compact electrodes;

The same or similar order may be expected for the rates of NO_3^- electrochemical elimination.

porous Ag and estimation of roughness factor by EIS

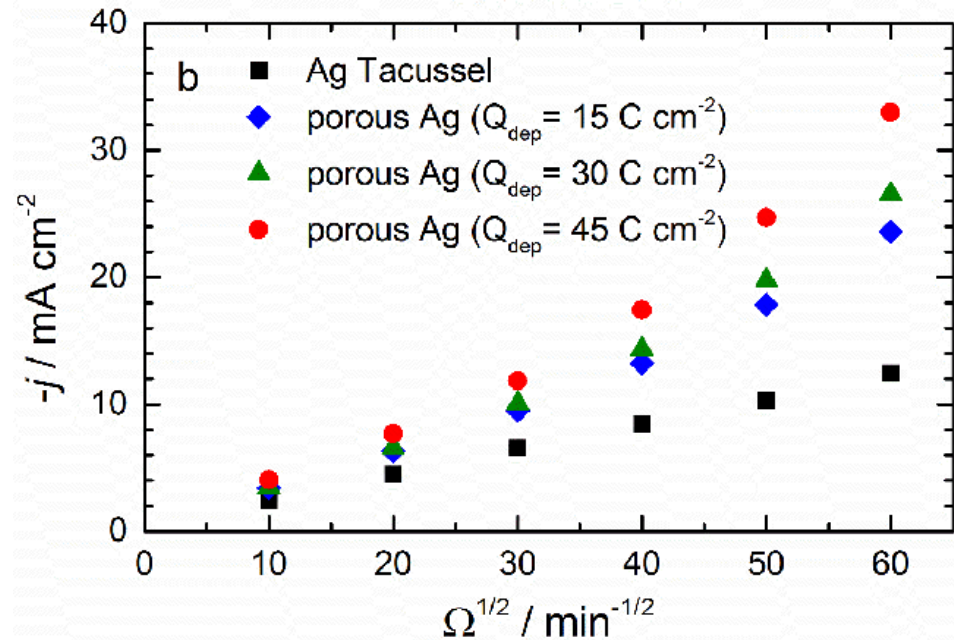
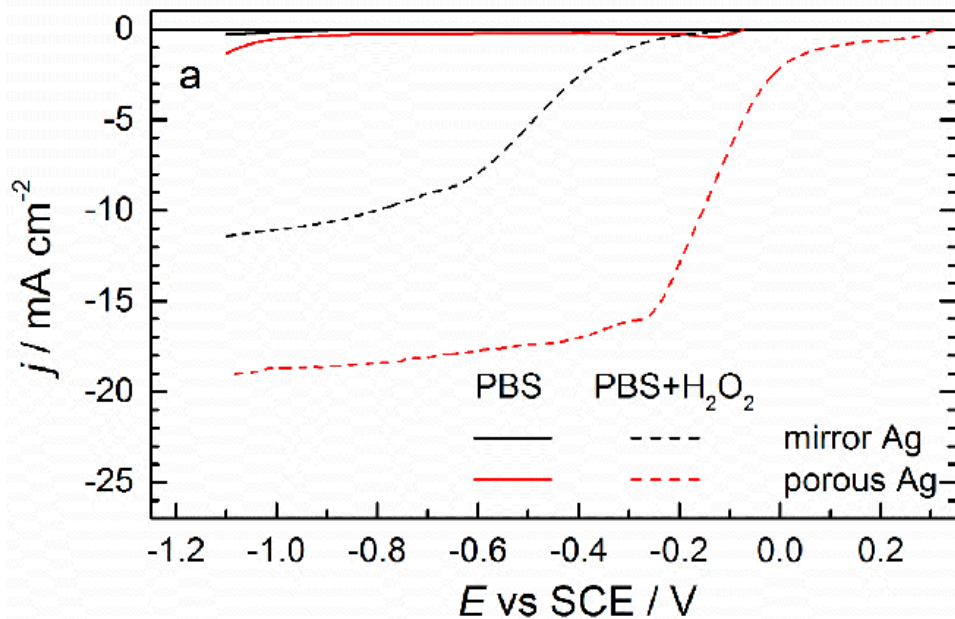


Bath: 0.03 M CH_3COOAg + 2.0 M $\text{CH}_3\text{COONH}_4$



Linear dependence of f_r on deposition charge

Electroactivity for hydrogen peroxide reduction



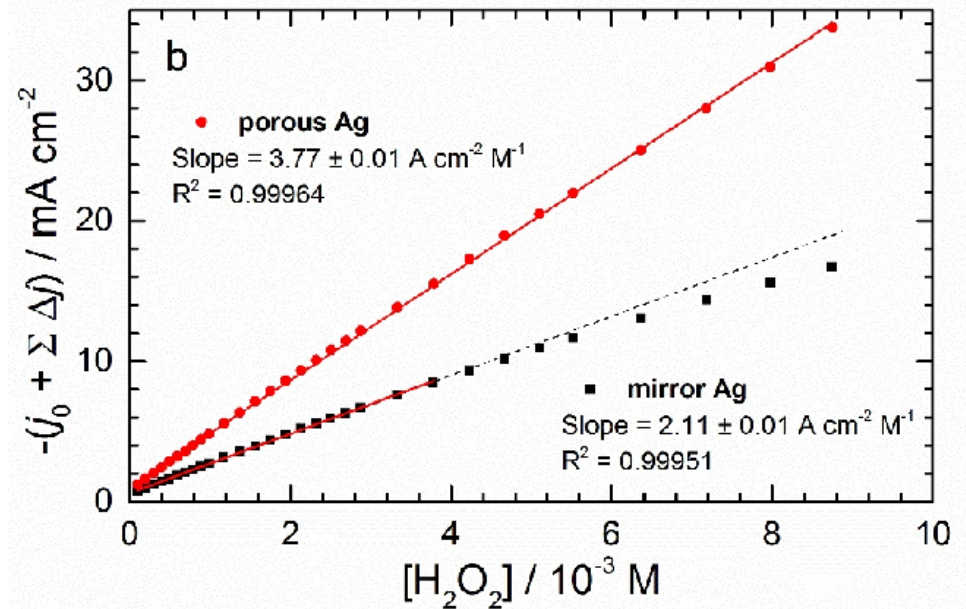
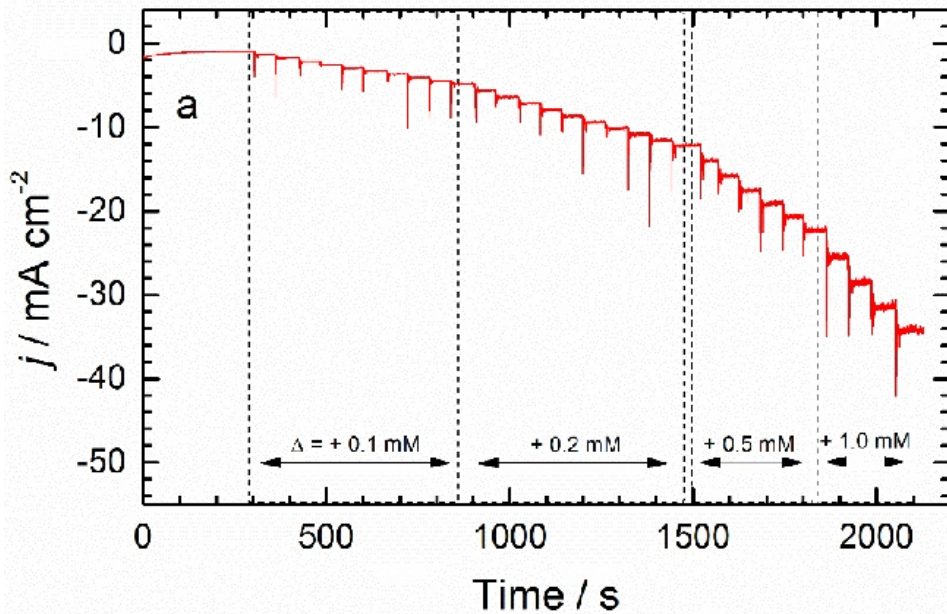
0.1 M KH₂PO₄ + 0.1 M K₂HPO₄ = **PBS**

5 mM H₂O₂ + 0.1 M KH₂PO₄ + 0.1 M K₂HPO₄ = **PBS + H₂O₂**

Current enhancement at porous electrodes: similar to that observed for ferricyanide reduction in alkali at Cu₇₀Ni₃₀ RDEs.

May result from more effective convection and/or solution perfusion (theory of **Porous Rotating Disk Electrodes**).

Calibration of Ag foam as amperometric sensor for H₂O₂



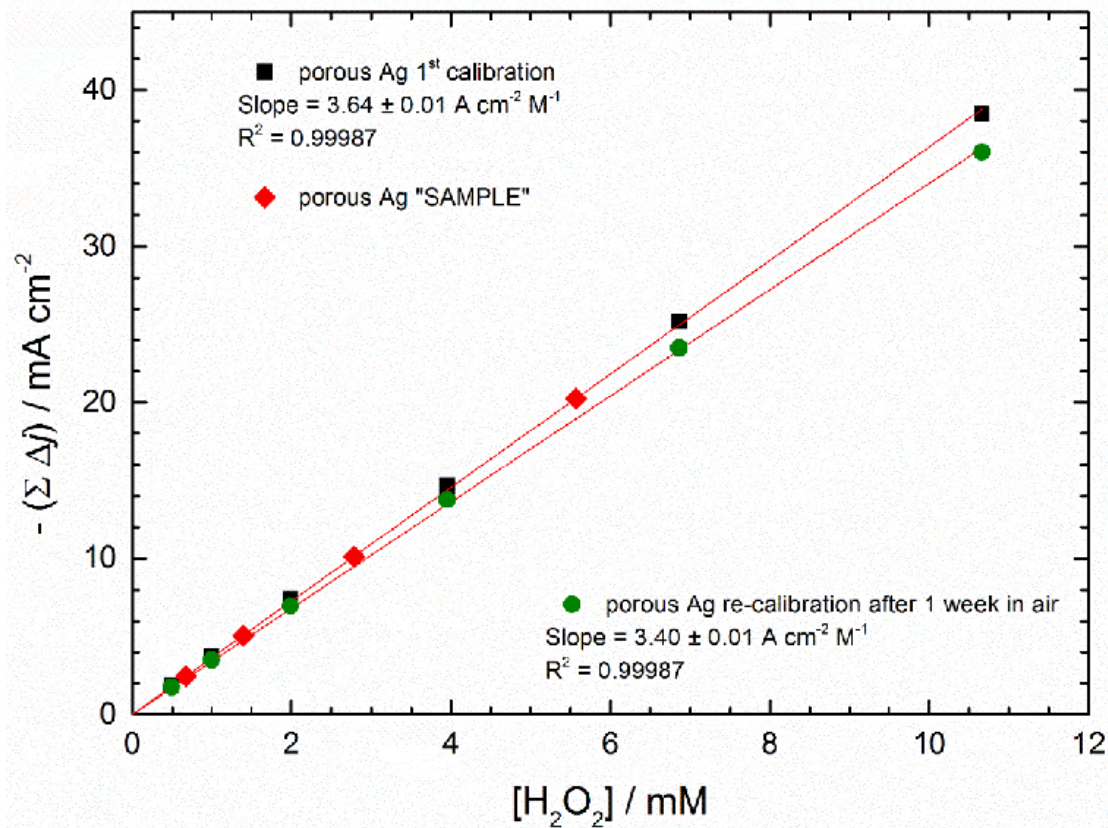
0.1 M KH₂PO₄ + 0.1 M K₂HPO₄, pH ca. 7

RDE speed: 2500 rev min⁻¹; E = -0.9 V vs SCE

H₂O₂ additions as indicated

	porous Ag •	mirror Ag ▪
sensitivity / A cm ⁻² M ⁻¹	3.77	2.11
LOD / μM	4.1	4.9
Linear range / mM	Up to 16	Up to 4-5

Reliability of porous Ag for H₂O₂ sensing



Experimental sequence:

1a) 1st calibration ■

1b) test the sensor response ◆
with 4 injections of known [H₂O₂] ("SAMPLE")

after 1 week in air



2) re-calibration ●

Conclusions

- The dynamic hydrogen bubbles template method allows deposition of several porous metals and alloys as large surface electrode materials;
- Despite the high deposition rate, Cu alloys can be deposited as crystalline solid solutions over a large range of compositions;
- Porosity includes macroscopic pores tens of microns large and a spongy or fluffy material;
- Electrochemical processes at these electrodes show a marked current enhancement as compared to compact electrodes even for diffusion-controlled processes;
- Due to their large surface area (f_r in the order of hundreds), porous materials show an **increased stability** in processes causing surface blocking by adsorption of reaction intermediates;
- 1st example: for electrochemical nitrate remediation, porous materials are **more efficient** (higher current density) and have **better selectivity** towards production of a single product (NH_3);
- 2nd example: porous Ag performs H_2O_2 detection better than flat Ag (benchmark):
response linearity over a **larger** concentration range
increased sensitivity, comparable detection limit
- Investigations in progress may allow extension to other metals and alloys for other applications.